Solar Powered Solid Oxide Fuel Cell with Thermoelectric Generator

Stephen Adavbiele

Ambrose Alli University, Nigeria

0086

The Asian Conference on Education 2013

Official Conference Proceedings 2013

Abstract

Durable, location independent, environmental-friendly sources of energy which allow for modular, few moving parts, low operating noise, high electricity generation efficiency and compact technology are highly desirable. Solid oxide fuel cells (SOFC) are promising for such energy system development, since they are energy efficient and, if pure hydrogen is used, have virtually no emissions of greenhouse gases except water and heat. However, the technology is still in the early phases of development due to lack of a design for single hydrogen fuel cells, and problems with hydrogen production and storage. In this study, an all year round operation home generator recovering its waste heat, integrated with photovoltaic panels supplying energy to split recyclable water (electrolysis) into hydrogen and oxygen has been put in place. The mathematical models of the unit as energy, charge, efficiency, activation and concentration losses of gases in channels were elaborated. The models gave necessary information for assessing and optimizing the design. The experimental results have demonstrated a remarkable energy generation and recovering with the integrated system, lower noise, possibility of achieving hydrogen economy and therefore clean environment.

Keywords: solar, recycled water, SOFC, TEGs, efficacy

1. Introduction

Since the problems with energy supply and use are related to global warming, environmental concerns such as air pollution, land destruction, and may include emission of radioactive substances; there is growing consensus that our approach to deriving and using energy must be changed. This in turn drives a renewed search for credible alternative energies and more efficient technologies [1]. Indeed, energy is one of the main factors that must be considered in the discussions of sustainable development. In response to the critical need for a cleaner energy technology, some potential solutions have evolved, such as solar and fuel cells [1].

Fuel cells generate direct current (DC) electricity, like photovoltaic (PV) panels, and heat through an electrochemical combination of gaseous fuel (hydrogen) and oxidant gas (oxygen from the air) through electrodes and via an ion conducting electrolyte without the need for direct combustion as an intermediate step. This gives much higher conversion efficiencies than conventional thermo mechanical methods or a battery because it is not limited by Carnot efficiencies [2-4]. However, unlike a battery, a fuel cell does not run down or require recharging. A fuel cell operates as long as both fuel and oxidant are supplied to the electrodes and without emission; is extremely attractive from an environmental point of view.

Solid oxide fuel cells (SOFCs) are a part of the family of fuel cell technologies, which are flexible in the choice of fuels such as hydrogen, natural gas, and other renewable fuels [5, 6]. The difference of solid oxide from other types of fuel cells is the catalyst that reacts with hydrogen and oxygen to form water, heat, and power. Solid oxide fuel cells use a solid, non-porous metal oxide, denoting the name solid oxide [7, 8]. SOFC technology is the most demanding from a material standpoint and is developed for its potential market competitiveness arising from the followings: First, they are composed of all-solid-state materials [4, 6]. Second, the cells can operate at temperatures as high as 1000°C, which enables high reactant activity and therefore facilitates fast electrode kinetics (large exchange currents) and reduced activation polarization. This is especially advantageous as precious platinum electro-catalysts are not required and the electrodes cannot be poisoned by carbon monoxide. As a result, carbon monoxide is a potential fuel in SOFCs. The only loss is the ohmic losses due to charge transport across components and component interfaces [9, 10]. Third, the solid state character of all SOFC components means the unit can be modular and that there is no fundamental restriction on the cell configuration. Fourth, the fuel cell itself has no moving parts, making it quiet enough to be installed indoors and its configuration allows a compact design without requiring expensive materials for production, so manufacturing costs could be reduced in the future. These advantages may enable SOFCs to be located anywhere as desired to eliminate the need for transmission lines, making the energy available where there is no grid electricity. SOFCs could provide higher power density, and simpler designs than fuel cells based on liquid electrolytes. SOFCs do not have problems with electrolyte management (liquid electrolytes, for example, which are corrosive and difficult to handle). SOFC can also provide high-quality waste heat for gas turbine, steam turbine and thermoelectric generator (TEG), warm the home or provide thermoelectric refrigeration and air conditioning without refrigerants harmful to the environment. SOFCs have a potential long life expectancy of more than 40000–80000 h [11].

The electrolysis process, which Sir William Grove invented in 1839 was reversed fifty years later, by scientists Ludwig Mond and Charles Langer (which they coined the fuel cell), to produce electricity [5]. Emil Baur, a Swiss scientist and his colleague Preis experimented with solid oxide electrolytes in the late 1930s, using such materials as zirconium, yttrium, cerium, lanthanum, and tungsten oxide, achieving the operation of the first ceramic fuel cell at 1000^0C in 1937 [5, 9]. By the late 1950s, research into solid oxide technology began to accelerate at the Central Technical Institute in Hague, Netherlands, Consolidation Coal Company, in Pennsylvania, and General Electric, in Schenectady, New York [6-13]. The promise of a high temperature cell that would be tolerant of carbon monoxide and use a stable solid electrolyte continued to draw modest attention. Researchers at Westinghouse, for example, experimented with a cell using zirconium oxide and calcium oxide in 1962 [12, 13]. More recently, climbing energy prices and advances in materials technology have reinvigorated work on SOFCs, and a recent report noted about 40 companies working on these fuel cells that include Global Thermoelectric's Fuel Cell Division, at the Julich Research Institute in Germany [14]. Venkatasubramanian et al [14], Rosendahl et al [15] and Brawn [16] reported work done on SOFC, with heat recovering thermoelectric generator (TEG), which shoot the efficiency of the system higher than 60%. Research work also continued to find a way to see if production of hydrogen can be integrated with the SOFC system. However, no attempt has been made to integrate SOFC with photovoltaic (PV) electrolysis and at the same time incorporate thermoelectric generator (TEG) in the system. A foray to achieve this is the essence of this presentation.

2. Materials and Method

A tripartite system as shown in Figure 1 is considered in this study, which is an integration of PV panel, an electrolysis compartment within the PV panel, (for hydrogen fuel production), eight layers of stacked SOFC in the vertical direction (from bottom-to-top); air-tight interconnect (current collector); air-side gas micro-channels, porous cathode, solid electrolyte, porous anode, fuel-side micro-channels, interconnect on fuel side and four TEGs. Figures 2c (i and ii) depicts the major components. The length of the SOFC is 128mm, width 100mm and height 80mm. The water vessel is made up of perplex glass with connected tubes, which lead away water into the PV-electrolysis panel and receive hydrogen and oxygen from the SOFC.

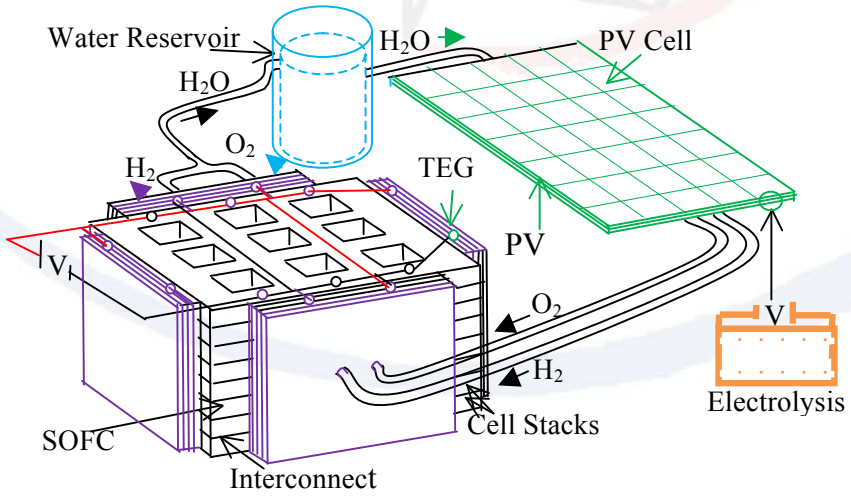

Figure 1: Components of the Electrolysis, Solid Oxide fuel Cell and TEG Integrated Unit.

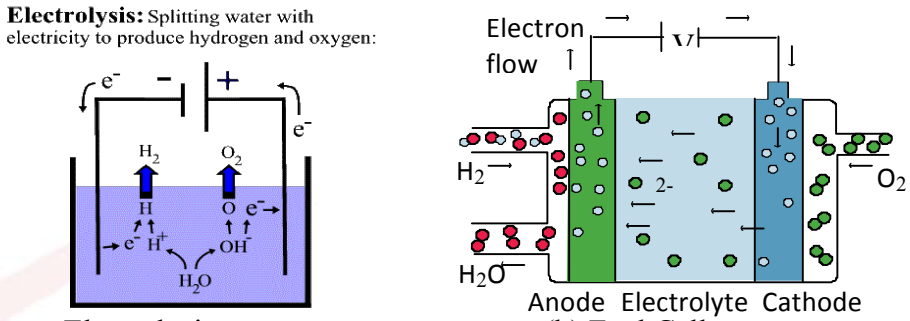

(a) Electrolysis (b) Fuel Cell

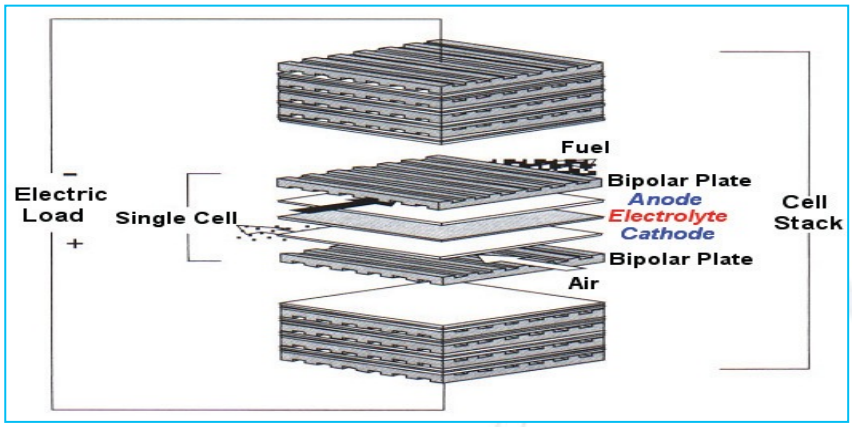

(i)

(ii)

(c) Cell Stack

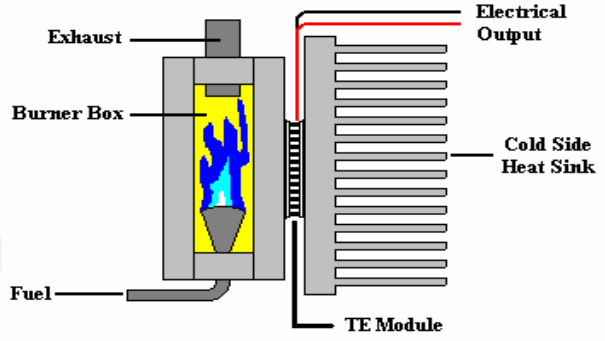

(e) TEG Module

Figure 2: Major Component of Solar Power SOFC with TEGs

Oxygen and hydrogen are introduced to the micro-channels of the SOFC via manifolds that would support a thin film structure to generate current. In the

circumstance, the materials involved in the construction are diverse in nature. The materials for the electrolysis of water, the fuel cell and TEG components are selected based on suitable electrical conducting properties required of these components to perform their intended functions; adequate chemical and structural stability at high temperatures encountered during operation as well as during fabrication; minimal reactivity and inter diffusion among different components and matching thermal expansion among different components are also considered [9, 17].

The PV panel is made of monocrystalline semi-conductors with a single photoelectrolysis nanoscale process: photon absorption in the PV creates a local electron-hole pair that electrochemically splits a neighboring water molecule. The semiconductor electrode is not in contact with the solution, but only air, so that corrosion problems cease; long lifetime is thus expected, the current density is reduced and the capital cost of electrolyzer is eliminated. The anode is made up of a combination of nickel and yttria stabilized zirconia, the cathode is made up of lanthanum strontium maganate and the electrolyte is of yttria stabilized zirconia. The cathode contact is lanthanum strontium chromate; the anode contact is nickel mesh and the sealing is with barium silicate glass. To increase voltage output to produce significant amounts of power, the SOFC elements, each including an anode, electrolyte, and cathode, are stacked (analogous to a multi-layered sandwich) with interconnecting plates between them that connect the anode of one cell to the cathode of the next cell in the stack to form the heart of a clean power generator. The cell frame is made up of doped lanthanum chromium ferrite ($LaCro_3$Fer22APU (JS-3), particularly suitable from its high electronic conductivity, its stability in the fuel cell environment and its compatibility with other cell components. The basic topology of the tubular design is retained and translated into planar geometries [18, 19]. Therefore, the cells are flat-plates bonded together and placed one on top of the other to form a stack as shown in figure 2c (i and ii) and hydrogen and air flow down channels in the bipolar plates. The cells are connected in electrical series to build a desired output voltage and can be configured in parallel to build up the current or combination of series-parallel or as single units, depending upon the type of applications. The number of fuel cells in a stack determines the total voltage, and the surface of each cell gives the total current.

The TEGs (figure 2d) attacked to the SOFC consist of semi-conductors and a compression assembly system [14, 15]. The compression assembly system aims to decrease the thermal contact resistance between the thermoelectric module and the SOFC surface. The size of the module used in the TEG is 12 mm thick by 120mm length and 80 mm in height. The module consists of 4 couples of p- and n-type Si-Ge elements. Sixteen modules are arranged around the fuel cell with a rectangular cross. At each side of the fuel cell, four modules each are electrically connected in series in each side of the fuel stack to increase the voltages and the current of the system is double by having the four modules connected to each of the other four modules in the three other sides of the fuel stack in parallel using Molybdenum electrodes by brazing method.

3. Theoretical Formulation and Analysis of the System

Electrolysis, SOFC and TEG modeling techniques have advanced significantly, with models at both micro-scales and macro-scales being developed. In SOFC and electrolysis of water, complex multi-physical and chemical phenomena interact with

transport processes. With SOFC, microscopic models are aimed at building better electrodes and electrolyte, while macroscopic models target stack optimization [19].

3.1: Assessment of the PV Hydrogen Fuel for the SOFC

The process of electrolysis of water must provide the energy for the dissociation plus the energy to expand the produced gases [17]. Both of these are included in the change in enthalpy. The chemical equation for electrolysis is:

Energy (electricity) + $2H_2O$ -> O_2 + $2H_2$

As water is not a very good conductor, in order for there to be a flow of charge all the way around the circuit, water molecules near the cathode are split up into a positively charged hydrogen ion, which is symbolized as H^+, and a negatively charged "hydroxide" ion, symbolized as OH:

H_2O -> H^+ + OH^-

The hydrogen atom meets another hydrogen atom and forms a hydrogen gas molecule:

H + H -> H_2,

and this molecule bubbles to the surface to form hydrogen gas. In this way, a closed circuit is created, involving negatively charged particles - electrons in the wire, hydroxide ions in the water. The energy delivered by the solar panel is stored by the production of hydrogen.

A detailed analysis of the electrolysis process makes use of the four thermodynamic potentials and the first law of thermodynamics. This process is presumed to be at 298K and one atmosphere pressure. The system's work and internal energy are:

$W = p\Delta v$ (1)

$\Delta U = \Delta H - p\Delta v$ (2)

where W is the work done; p, pressure; Δv, change in volume; ΔU, change internal energy and ΔH, change in enthalpy – $p\Delta v$. This change in internal energy must be accompanied by the expansion of the gases produced, so the change in enthalpy represents the necessary energy to accomplish the electrolysis. However, it is not necessary to put in this whole amount in the form of electrical energy. Since the entropy, $T\Delta S$, increases in the process of dissociation, the amount $T\Delta S$ can be provided from the environment at temperature, T. The amount which must be supplied by the PV solar panel is actually the change in the Gibbs free energy, ΔG:

$\Delta G = \Delta H - T\Delta S$ (3)

The utility of the Gibbs free energy is that it is a measure of the amount of energy, which must be supplied to get the process to proceed.

Calculation of the theoretical (maximum) volume, v of the hydrogen produced, in cubic meters, from the other data for the current, I and the time, t using Faraday's First Law is provided by the equation [4]:

$v_{theoretical} = (R\ I\ T\ t) / (F\ p_a z)$, (4)

where R=8.314 Joule/(mol Kelvin), I = current in amps, T is the temperature in Kelvins (273 + Celsius temperature), t = time in seconds, F = Faraday's constant = 96485 Coulombs per mol, p_a = ambient pressure = about 1 x 10^5 Pascals (one Pascal =

1 Joule/meter^3), z = number of excess electrons = 2 (for hydrogen, H_2), 4 (if oxygen production is being measured).

Finally, calculation of the efficiency of the electrolysis by comparing the volume produced to the theoretical maximum volume yields:

Efficiency (in %) = 100 x $V_{produced}$ / $V_{theoretical}$

(5)

3.2: Chemistry and Thermodynamics of the SOFC.

The physical-chemical transport phenomena within SOFC are complex, and so are the corresponding mathematical and numerical methods presently employed [19]. These include convection-diffusion of multi-species gas mixtures in micro-channels and porous media, heat and mass transfer due to electrochemical reactions and associated Ohmic heating, as well as kinetic (activation) terms. In SOFC, the ideal electric potential is a function of the fuel and oxidant concentrations, temperature, and pressure. The actual potential is less than the theoretical value due to kinetic, mass transfer and electrical losses. Current density is dependent on both voltage and cell resistance. Sources and sinks of mass, species and heat, are a function of current density. Thus the transport problem is fully coupled, that is, mass transfer in H_2 and O_2 channels and porous media; heat transfer in all constituent materials; electrochemical reactions at interfaces between electrolyte and electrodes; electronic and ionic charge transfer through solid and porous media. Convective heat transfer is the dominant transfer mechanism in the micro-channels, while conduction is important in the solid materials; i.e. the problem is one of so-called conjugate heat transfer.

At the fuel cell, the positive anode will cause the negatively charged hydroxide ion (OH^-) to travel across the container to the anode, where the extra electron that the hydroxide stole from the hydrogen atom earlier is removed, and then the oxygen can react violently with the hydrogen gas, such that the hydrogen burns, or combusts, with the oxygen to form water and heat, generating electricity and according to the chemical reaction:

$2H_2 + O_2 \rightarrow 2H_2O$ + energy (heat).

Understanding the impacts of variables such as temperature, pressure, and gas constituents on performance allows for the optimization of the design of the modular fuel cell units as well as the maximization of the performance of systems applications. A logical first step in understanding the operation of a fuel cell is to define and determine its ideal performance; losses arising from non-ideal behavior can be calculated, and then deducted from the ideal performance to describe the actual operation [4]. This is provided by the chemistry and thermodynamics of the reaction as follow:

Chemistry

Anode side: $2H_2 \Rightarrow 4H^+ + 4e^-$ and

at the cathode side: $O_2 + 4H^+ + 4e^- \Rightarrow 2H_2O$

Net reaction: $2H_2 + O_2 \Rightarrow 2H_2O$

Thermodynamics

$H_2+½O_2=H_2O$+energy, where the energy is:

$Energy=\Delta H_{rev}=\Delta G_{rev}+T\Delta S_{rev}$

(6a)

$$\Delta G = (\Delta H_0)\ H_20 - T(S\ H_2O\text{-}S\ H_2\text{-}0.5S\ O_2)$$

(6b)

$$\eta_f = \frac{\Delta G_{rev}}{\Delta H_{rev}} = 1 - \frac{T\Delta S_{rev}}{\Delta H_{rev}} = \frac{\Delta G^0}{\Delta H^0} + \frac{RT}{\Delta H^0} In \prod_k \prod P_k^{vk}$$

(7)

ΔG_{rev} is the maximum useful work associated with a chemical reaction, ΔH is the maximum heat associated with a chemical reaction at rev reversible conditions and η_f is fuel cell efficiency. There are many ways in which the Gibbs function can change: temperature, pressure, amount of material, surface area and elastic stretch:

$$\mathrm{d}G = -S\,\mathrm{d}T + V\,\mathrm{d}P + \sum \mu_i\,\mathrm{d}n_i + \gamma\,\mathrm{d}A + f\,\mathrm{d}l$$

(8a)

If everything is kept constant (for constant temperature, pressure, area and length), except material, then the changes in the Gibbs function is the result of the changes in the composition of the system:

$$\mathrm{d}G = \sum \mu_i\,\mathrm{d}n_i$$

(8b)

If the Gibbs function is known in terms of pressure, temperature and amount of material (T, P, n), then, with a variety of partial derivatives, all other thermodynamic properties can be calculated. If the Helmholtz function is expressed in terms of (T, v, n), whwre n stands for number of moles, then we have access to all the other parameters also. However, if we only know G in terms of (T, v, n), then we cannot perform the necessary differentials.

A detailed analysis of the fuel process makes use of the same thermodynamic potentials, but the process of electrolysis reversed in SOFC. In comparing the fuel cell process to its reverse reaction, electrolysis of water, it is useful to treat the enthalpy change as the overall energy change. So in the electrolysis/fuel cell pair where the enthalpy change is 285.8 kJ, 237.1 kJ of energy has to be put in to drive the electrolysis and the heat from the environment will contribute $T\Delta S$=48.7 kJ to add up to it. Going the other way in the fuel cell, 237.1 kJ as electric energy is produced, but have to dump $T\Delta S$ = 48.7 kJ to the environment. For this ideal case, the fuel energy is converted to electrical energy at an efficiency of 237.1/285.8 x100% = 83%. This is far greater than the ideal efficiency of a generating facility which burned the hydrogen and used the heat to power a generator. Although real fuel cells do not approach this ideal efficiency, they are still much more efficient than any electric power plant which burns a fuel. An interesting difference between the fuel cell and the combustion process is that many fuel cells attempt to release the higher enthalpy of reaction, whereas combustion usually releases the lower enthalpy (or internal energy) of reaction.

When the substance is a charged particle (such as an electron or an ion) the response of the particle must be included to an electrical field in addition to its chemical potential. This is called the electrochemical potential, $\overline{\mu}_k$ given as [4]:

$$\overline{\mu}_k = \mu_k + z_k F \phi_k$$

(9a)

μ is the chemical potential, z is the charge on the particle, F is Faraday's constant and ϕ is the field under consideration. At reversible reaction in quilibrium,

$$\sum_k \nu_k \mu_k = 0$$

(9b)

$$E_{rev} = E_c - E_a = \frac{1}{2F}\left[\mu H_2 + \tfrac{1}{2}\mu O_2 - \mu H_2 O\right]$$

(10)

For hydrogen fuel and oxygen, the free energy is:

$$\Delta G^0 = \mu^0 H_2 O - \mu^0 H_2 - \tfrac{1}{2}\mu^0 O_2$$

(11)

where E_{rev} is the reversible electromotive force, E_c, the electromotive force at the cathode and E_a, the electromotive force at the anode. The superscript, o stands for values obtained at atmospheric conditions.

For an ideal gas, integration of the expressions for the dependence of amount of material on the Gibbs function, leads to the following relationship [4]:

$$\Delta G = \Delta G^{\circ} + RT \ln Q$$

(12)

Q contains all of the activity of terms of the reactants and products, each raised to its stoiochiometric coefficient. $\Delta G = -nFE_{rev}$ and $\Delta H = -nFE_{therm}$. The relation between cell potential, E and free energy then leads to the following equation:

$$-nFE = -nFE^{\circ} + RT \ln Q$$

(13a)

If the reaction is proceeding at the electrodes, there will be a reduction in the concentration of reactants. The Nernst equation describes effects of reduction in reactant concentration. Rearranging equation (13a) gives the Nernst Equation:

$$E = E^{\circ} - \frac{RT}{nF} \ln Q$$

(13b)

When all participants have unit activity (a=1), then Q=1 and lnQ=0; and $\Delta G = \Delta G^o$, reaction proceeds, Q changes, until finally $\Delta G = 0$ and the reaction stops. This is equilibrium. The chemical equation of reactants and products is usually given by the reaction quotient:

$$Q = \frac{a_C^y \, a_D^z}{a_A^w \, a_B^x}$$

(14)

which always has products in the numerator and reactants in the denominator and explicitly requires the activity of each reaction participant. Each term is raised to the power of its stoichiometric coefficient; terms involving solids, pure liquids, and solvents are left out, solutes appear as the concentration (in moles) and gases appear with their partial pressure. Substituting back equation (14), with water as the product and hydrogen and oxygen as the reactants along with their pressires, into equation (13b),

$$E_{rev} = -E^0 + \frac{RT}{2F} In\left[\frac{pH_2 . pO_2^{\frac{1}{2}}}{pH_2O}\right]$$

$$= \frac{RT}{2F}\left\{InK_p - In\left(\frac{pH_2O}{pH_2 pO^{0.5}}\right)\right\}$$

(15)
This Nernst reversible voltage (E_{rev}) is the open-circuit voltage of the SOFC cell when the current density is zero. E is the electromotive force (emf) or reversible open circuit voltage (V). $E_0 = 1.1$ V is the standard potential (the emf at standard pressure), K is the universal gas constant and p is the partial pressure.

The efficiency of an actual fuel cell is often expressed in terms of the ratio of the operating cell voltage to the ideal cell voltage:

$$\eta_{thermal} = \frac{E_{actul}}{E_{ideal}} x \frac{I}{I/0.83} = \frac{0.83 E_{actual}}{E_{ideal}}$$

(16)
The output voltage, V_{fc} of the SOFC is given by Stambouli and Traversa [5]:

$$V_{fc} = E_{rev} - V_{act} - V_{con} - V_{ohmic}$$

(17)
where V_{act} is the activation loss, V_{con} is the concentration loss, and V_{ohmic} is the ohmic loss.

Chemical reactions, including electrochemical reactions, must overcome energy barriers, called activation energy, for the reaction to proceed. This leads to activation polarization. The activation loss is given by the Butler–Volmer equation [20-221]:

$$I_{fr} = I_f - I_r = I_o \left[\exp\left(\frac{\alpha_a nF}{RT} \right) V_{act} - \exp\left(-\frac{\alpha_c 2nF}{RT} \right) V_{act} \right]$$

(18)
where I_0 is the exchange current, α_a is the coefficient of anode charge transfer, α_c is the coefficient of cathode charge transfer and n = 2 is the number of moles of electrons transferred.

The concentration voltage loss occurs due to the mass transfer resistance to the flow of the reactants and the products through the porous electrodes. Concentration voltage loss can be calculated as [21, 23]:

$$V_{con} = \frac{RT}{nF} In\left(\frac{C_s}{C_b} \right)$$

(19a)
The potential difference (ΔE) produced by a concentration change at the electrode is called the concentration polarization:

$$\Delta E = \eta_{con} = \frac{RT}{nF} In \frac{C_s}{C_b} = \frac{RT}{nF} In\left(1 - \frac{i}{i_L} \right)$$

(19b)
where C_s is the concentration at the triple-phase boundary (tpb), where the gas, electrolyte, and electrode meet; C_b is the bulk concentration of reactant; i, current, L limiting and n is the number of moles of electrons participating in the reaction (in this case, n = 2).

The Ohmic losses occur because of the resistance to the flow of ions in the electrolyte and the resistance to the flow of electrons through the electrode materials. The inherent resistance of a fuel cell governed by the change in cell temperature is given by [21]:

$$V_{ohmic} = \left[\gamma \exp\left(\beta\left\{\frac{1}{T_o} - \frac{1}{T}\right\}\right)\right] I_{fr} = rI_{fr}$$

(20)

where T is the fuel cell temperature; T_0 = 973 K, γ = 0.2 Ω, and β = −2870 K are the constant coefficients of the fuel cell; and r is the internal resistance of the SOFC.

The performance of the fuel cell depends on the electrochemical reactions that take place at the tpb. A relationship that governs the mass flow rate conservation in the fuel cell is given by [22]:

$$\frac{v}{RT}\frac{dp}{dt} = N_x^{in} - N_x^o - N_x^r$$

(21)

where v is the volume of the fuel cell electrode, N^{in} is the input mole flow rate, N^o is the output mole flow rate, N^r is the mole flow rate reacted, p is the partial pressure, and x is the species. The electricity generated from the electrochemical reaction inside the fuel cell is given by [22]:

$$I_{fc}^r = \frac{4FN_x^r}{n}$$

(22)

where n =2 for hydrogen and water and is 1 for oxygen

Irreversible losses, fuel depletion, and fuel utilization serve to reduce fuel-cell efficiency. Therefore, the component efficiencies in the system are:

- Reversible efficiency - theoretical efficiency: $\eta_{rev}=\Delta G/\Delta H$
- Voltage efficiency- efficiency based upon operating voltage: η_{volt} =E/Erev
- Faradaic efficiency: η_F=i/iF
- Utilization efficiency - reactant utilization: the fuel utilization is defined by $\eta_u=n_{reacted}/n_{total} = \frac{H_2, consumed}{H_2 + O_2}$
- Auxiliary loads - parasitic power consumption: $\eta_a=1-P_{pl}/P_{total}$

The total efficiency is multiplicative and expressed, therefore, as:

$$\eta_{total}=\eta_{rev} .\eta_{volt} .\eta_F .\eta_u .\eta_a$$

(23)

In general, the cell energy balance states that the enthalpy flow of the reactants entering the cell will equal the enthalpy flow of the products leaving the cell plus the sum of three terms: (1) the net heat generated by physical and chemical processes within the cell, (2) the direct current, DC power output from the cell, and (3) the heat loss from the cell to its surroundings. The first general purpose fuel cell model was a Nernst-limited model designed to compute the maximum attainable fuel cell voltage as a function of the cell operating conditions, inlet stream compositions, and desired fuel utilization. As operation deviates from the set point conditions at a reference state, a voltage adjustment is applied to account for perturbations. Separate voltage adjustments are applied for current density, temperature, pressure, fuel utilization, fuel composition, oxidant utilization, oxidant composition, cell lifetime, and production year [8].

3.3: Thermodynamics of the Thermoelectric Generator to Recover SOFC Waste Heat

The efficiency of a thermoelectric generator (TEG) is the amount of electrical power generated, P_{elec} for a given amount of heat input, P_h, that is, $\eta_{TE} = P_{elec} / P_h$. This efficiency can be calculated as a function of the hot-side temperature, T_h, the cold-side temperature, T_c, and the dimensionless figure of merit, ZT as [14, 15, 24]

$$Q_{\max} = \frac{S_m^2 T_c^2 N_c}{\rho\lambda} + \frac{T_c - T_h}{\lambda / 2k_m N_c}$$

(24)

$$COP_{generator} = \eta_{TE} \cdot \frac{Q_{TE}}{Q_h} = COP_C \left[\frac{\sqrt{1+ZT_m} - 1}{\sqrt{1+ZT_m} + \frac{T_c}{T_h}} \right] \frac{Q_{TE}}{Q_h}$$

(25)

where $COP_C=(T_h-T_c)/T_h$ is the Carnot COP , $\eta_{TE} = COP_C \left[\frac{\sqrt{1+ZT_m} - 1}{\sqrt{1+ZT_m} + \frac{T_c}{T_h}} \right]$ and $ZT_m = \frac{S^2\sigma}{k} T = \frac{\sigma S^2}{(k_p + k_n)} T = \frac{S^2}{k\rho} \frac{(T_c + T_h)}{2} = \frac{\sigma \frac{\Delta V}{\Delta T}}{k} T$= 1.2 to 1.8 with 1.6 as viable figure; $T_m=1/2(T_h+T_c)$ and T_h and T_c are the hot and cold temperatures of TE module, respectively. The total efficiency of the generator can be defined as:

$$\eta_g = \eta_{he}.\eta_h.\eta_e$$

(26)

where: η_{he} is the efficiency of heat exchange of the generator η_h the ratio of heat flux through the elements in the modules to that from the inner shell to outer shell and η_e the thermoelectric conversion efficiency of the elements. The following are design specifications for the thermoelectric module: maximum difference in temperature, $dT_{max} = 10.5^0C$, $p_{max}=11$Watts, Seebeck's co-efficient, S =2.0 x 10^{-4} V/K; resistance, figure of merit, z=0.002346, ρ=1.10 x 10^{-3}ohm-cm and thermal conductivity, k_p=1.55 x 10^{-4} watts/m-K.); ρ, resistance (ohms) of the semiconductors; σ, electrical conductivity; k_p; material thermal conductivity for p-type and k_p, thermal conductivity for n type semi-conductor and R, resistance, in Ω of the system. Δt stands for change in temperature.

5. Results and Discussion

A model of the system was built and test run under laboratory conditions. Input water was distilled to ensure impurities is reduced to the barest minimum. A two month period was used in winter and summer respectively to determine these seasonal effect on performance and values averaged over the period. Digital instrumentations were used to gather data, which were assessed by the formulae presnted above. Obtained results are presented in tables 1-3 and figures 3-6 depict the characteristic perfomance.

Table 1: Photo-Electrolysis for Hydrogen Production

Time	Energy required for H_2O Electrolysis					
t Mins	T K	P_{panel} W	ΔH J	TΔS J/K	ΔG J	η_{Elect}
30	303.0	49.5	290.6	5.0	285.7	0.983
60	305.0	49.8	292.5	5.0	287.6	0.983
90	307.0	50.2	294.5	5.0	289.5	0.983
120	309.0	50.5	296.5	5.1	291.3	0.983
150	317.0	51.8	304.1	5.2	298.9	0.983
180	320.0	52.3	306.9	5.2	301.7	0.983
210	321.0	52.5	307.9	5.3	302.6	0.983
240	320.5	52.4	307.4	5.2	302.2	0.983
270	319.0	52.1	306.0	5.2	300.8	0.983
300	318.0	52.0	305.0	5.2	299.8	0.983
330	316.3	51.7	303.4	5.2	298.2	0.983
360	313.0	51.2	300.2	5.1	295.1	0.983
390	311.0	50.8	298.3	5.1	293.2	0.983
420	309.0	50.5	296.4	5.1	291.3	0.983
450	307.0	50.2	294.5	5.0	289.5	0.983
480	305.0	49.8	292.5	5.0	287.6	0.983

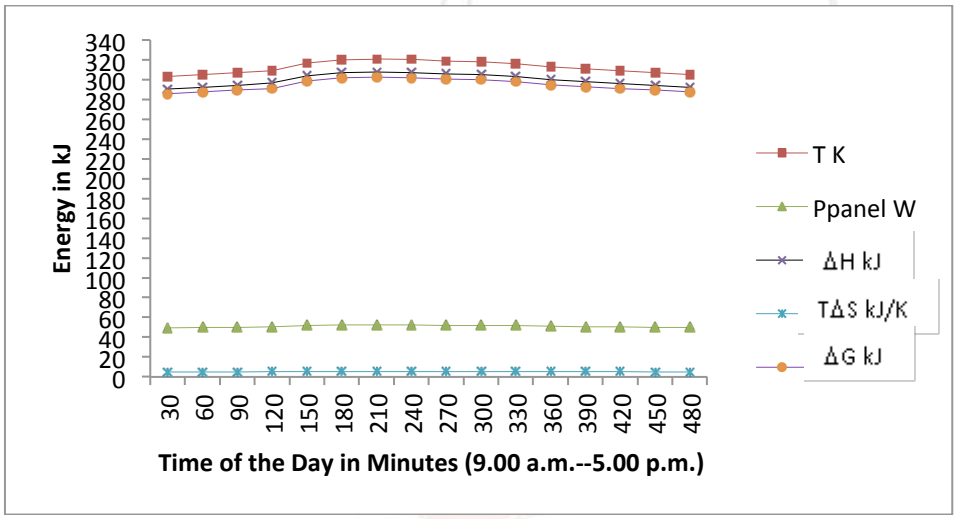

Figure 3: Energy Required for H_2O Electrolysis

The first step was to determine the effect of solar energy trapping on the system outputs. From table 1 and figure 3, it comes out that varying solar insolation vary the amount of the H_2 input yield, which has an impact on the total plant power as well as the electricity generated by the thermoelectric device. The next step was to determine the energy production in the SOFC as in table 2 and figure 4.

Table 2: Thermodynamics of SOFC

$H_2 + ½O_2 \rightarrow H_2O$ 1 bar reactant pressure (standard conditions)							
Temp in ^0C	**H_2O**	**ΔH (kJ/mol)**	**ΔG (kJ/mol)**	**$\eta_{theoretical}$**	**E (V)**	**E_{rev} (V)**	**$\eta_{thermal}$**
25	LHV (vapor)	-241.8	-228.6	94.5	1.253	1.185	0.785
	HHV (liquid)	-286.0	-237.3	83.0	1.482	1.229	0.688
80	LHV	-242.3	-226.2	93.3	1.256	1.172	0.774
	HHV	-283.8	-233.7	92.2	1.471	1.212	0.684
130	LHV	-242.8	-223.9	92.2	1.258	1.160	0.765
	HHV	-282.1	-230.4	81.7	1.462	1.195	0.678
200	LHV	-243.8	-219.1	89.8	1.259	1.131	0.746
400	LHV	-245.0	-210.2	83.1	1.267	1.119	0.733
600	LHV	-247.2	-198.1	80.1	1.277	1.023	0.665
800	LHV	-248.3	-186.3	75.3	1.285	1.017	0.657
1000	LHV	-249.4	-175.8	70.5	1.288	0.908	0.585

Where HHV is higher heat value (liquid state) and LHV is lower heat value (gaseous state)

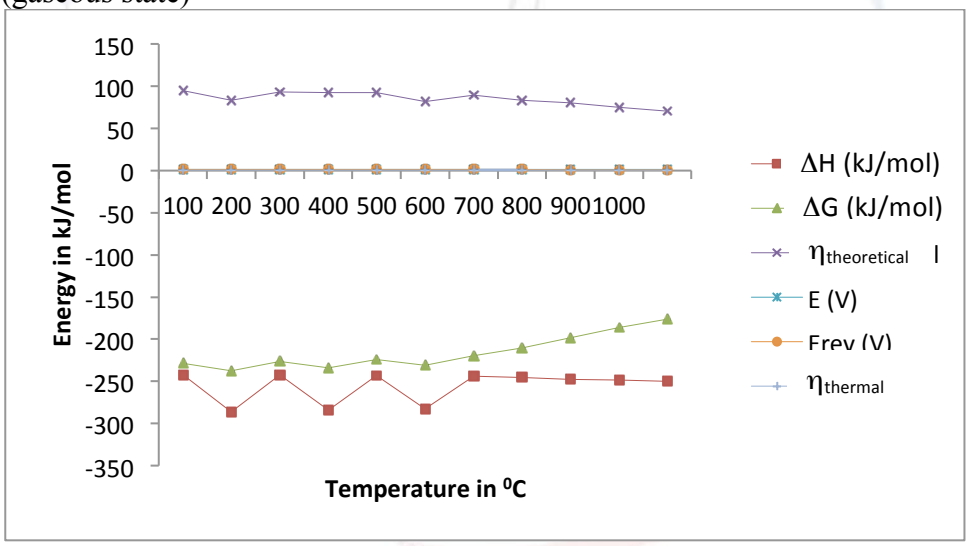

Figure 4: Energy of SOFC as a Function of Temperature

There is a marked difference between the results obtained at low temperature as indicated by the zigzag lines and at high temperature where the energy released appears linear. This is because at the low temperature part of the fuel is still in liquid state yielding both the higher and lower heating values of energy. At about 700^0C upward, figure 4 shows that while the energy released by the fuel continues to increase; there is marked drop in the available energy and the efficiencies (theoretical and thermal) of the system. However, there is only slight change in the voltage, which decreases as well.

Table 3: Solar Based S0FC/TEG Power Generation

Time	Energy released by SOFC					Energy recovered in TEG		Total energy	Relative Efficiency with and without TEG	
t Mins	T K	ΔH kJ	TΔS kJ/K	ΔG kJ	P_{SOFC} W	dT_{max} K	P_{TEG} W	P_{SOFC} + P_{TEG}	η_{SOFC}	$\eta_{SOFC+TEG}$
30	715	463.3	116.9	346.4	89.3	5.1	1.3	90.6	0.258	0.262
60	823	533.3	134.5	398.8	102.7	6.0	1.4	104.1	0.258	0.261
90	882	571.5	144.1	427.4	110.1	6.4	1.5	111.6	0.258	0.261
120	934	605.2	152.6	452.6	116.6	6.7	1.6	118.2	0.258	0.261
150	979	634.4	160.0	474.4	122.2	7.0	1.7	123.9	0.258	0.261
180	1323	857.3	216.2	641.1	165.2	7.2	2.3	167.5	0.258	0.261
210	1270	822.9	207.6	615.3	158.5	7.3	2.2	160.7	0.258	0.261
240	1114	721.9	182.1	539.8	139.1	7.2	2.0	141.1	0.258	0.261
270	1018	659.7	166.4	493.3	127.1	6.9	1.8	128.9	0.258	0.261
300	991	642.2	162.0	480.2	123.7	6.8	1.8	125.5	0.258	0.262
330	945	612.4	154.4	458	118.0	6.6	1.7	119.7	0.258	0.261
360	926	600.0	151.3	448.7	115.6	6.4	1.6	117.2	0.258	0.261
390	903	585.1	147.6	437.5	112.7	6.2	1.6	114.3	0.258	0.261
420	897	581.2	146.6	434.6	112.0	6.0	1.6	113.6	0.258	0.261
450	834	540.4	136.3	404.1	104.1	5.5	1.5	105.6	0.258	0.261
480	773	500.9	126.3	374.6	96.5	5.2	1.4	97.9	0.258	0.261

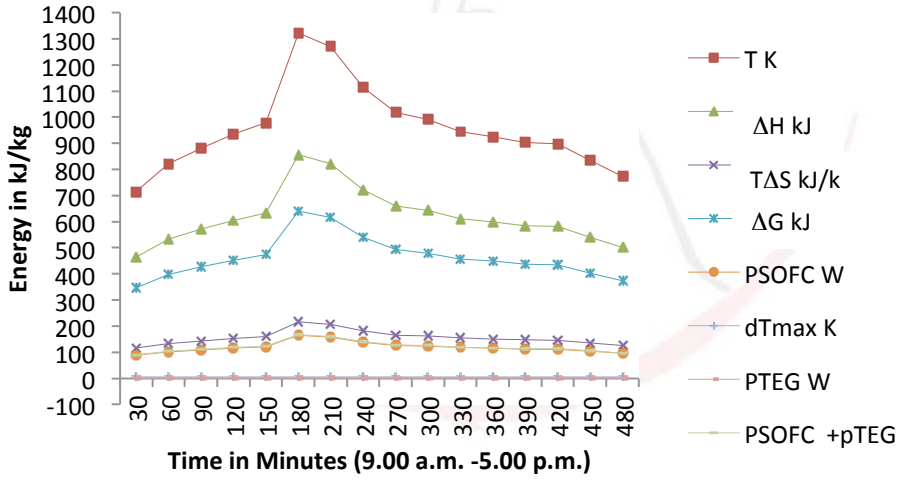

Figure 5: Energy Released by SOFC and Recovered by the TEG

The thermodynamic analysis as shown in figure 5 indicates that the SOFC with TEG has essential advantage as the total energy tends to be higher, thereby increasing the conversion of chemical energy of hydrogen into electrical energy. Again, the performance of the combined unit shows that this is dependent on the solar insolation; lower in the morning and evening than the afternoon. . The obtained results show that a remarkable energy can be generated and recovered from combining the photoelectrolysis with SOFC and TEGs. The thermodynamic analysis shows the SOFC with TEG has essential advantage as the total energy tends to be higher, thereby increasing the conversion of chemical energy of hydrogen into electrical energy. These observations can have important implications for the development of

the integrated unit with enhanced performance in this part of the world where seasonal temperature is above 30^0C (303K).
Finally, all the efficiencies of the electrolysis, SOFC without TEG and SOFC with TEG were computed and presented in figure 5.

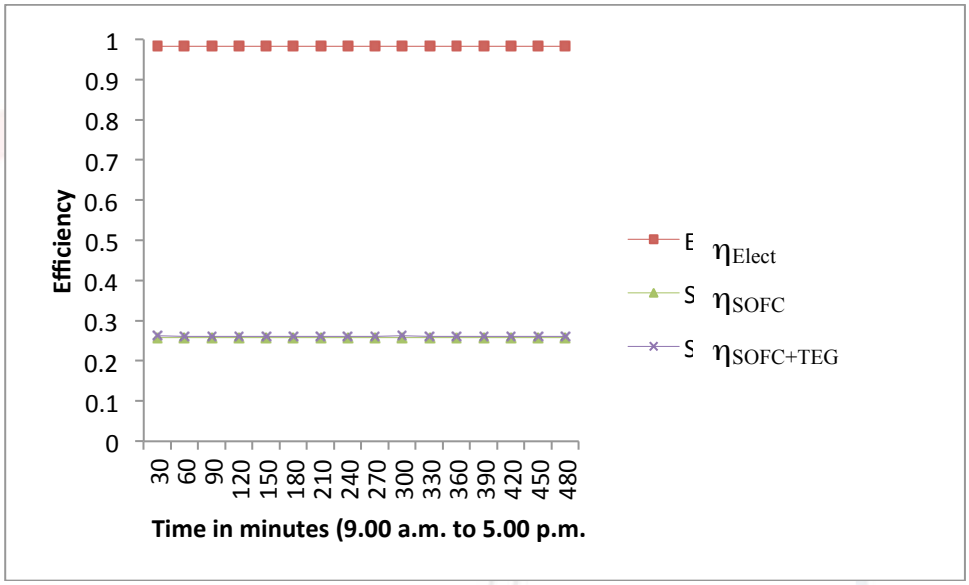

Figure 6: Comparative Efficiency of the Electrolysis, SOFC and SOFC+TEG Processes

From figure 6, it is found that the time and therefore, temperature dependence of the three components has a significant effect on the power, efficiency and optimal energy variables; increasing the temperature difference will always improve the power and efficiency. However, because of the effects of temperature dependence of the components, with the increase of temperature difference, the power improves more and more slowly while the efficiency remains constnt. From figure 5, where the efficiency of electrolysis process is estimated to be a constant value of 98.3 per cent, the SOFC with TEGs recorded maximum efficiency of 25.8; apart from this value, their combined efficiency stood at average value of 26.1.

6. Conclusion

The main achievement of this study is the development of a modular SOFC unit that is powered by a photovoltaic solar panel, has TEGs attached and can be used for future research. The mathematical models of the unit as energy, charge, efficiency, activation and concentration losses of gases in channels were elaborated. The models gave necessary information for assessing and optimizing the design. Analysis indicated that the performance of the entire system is strongly dependent on intensity of solar insolation; lower in the morning and evening than the afternoon.
In this part of the world, the experimental results have demonstrated a remarkable energy generation and recovering with the integrated unit, which could have important implications for the development of a unit with enhance performance. It is similarly critical that the technologies be demonstrated to perform and achieve the projected performance targets and demonstrate long life.

References

Adavbiele, A.S. and Aasa, S.A. (2012) Integrated flat plate solar thermoelectric system, European Journal for Scientific Research, UK. 76 (2) 253-270

Appleby, A.J. (1996). Fuel cell technology: Status and future prospects. *Energy.* 21 (3). 521-653.

Appleby, A.J. and Foulkes, F.R. (1993) Fuel cell handbook, 7th Edition, Van Norstand Reinhold, New York, N.Y., . Republished by Krieger Publishing Company, Melborne, FL.

Beale, S.B; Dong, W; Zhubrin, S.V. and Boersma, R.J. (2001). Calculations of ransport phenomena in stacks of solid-oxide fuel cells, *Proceedings, ASME International Mechanical Engineering Congress and Exposition*, IMECE2001/PID-25615, New York, November 11-16.

Braun, R. J; Klein, S. A. and Reindl, D. T. (2001). Assessment of solid oxide fuel cells in building applications. Phase 1: Modeling and preliminary analyses. Solar Energy Laboratory University of Wisconsin-Madison Madison, WI 53706. November.

Brawn, R. (2011). Report from the Solar Energy Laboratory. University of Wisconsin-Madison, WI. February 2002 (http://sel@sel.me.wisc.edu/). Global Thermoelectric Inc. Annual report 2001. Assessed on 21th November.

Ford, J.C. (2006). An enhanced transient solid oxide fuel cell performance model. A Thesis Presented to the Academic Faculty in partial fulfilment of the requirements for the degree master of science in Mechanical Engineering, Georgia Institute of Technology. December

Gebregergis, A. (2009) Solid Oxide Fuel Cell Modeling. IEEE Transactions on Industrial Electronics, 56 (1). January. 139-148

Iwata, M; Hikosaka, T; Morita, M; Iwanari, T; Ito, K; Onda, K; Esaki, Y; Sakaki, Y. and Nagata, S. (2000). Performance analysis of planar-type unit SOFC considering current and temperature distributions, Solid State Ionics, Journal of Energy: Cambridge, MA, USA 132 (3). Jul.. 297–308.

Kee, R. J. and Huayang Zhu. Editors (2004). Solid-oxide fuel cells (SOFC) with hydrocarbon and hydrocarbon-derived fuels. Report of the DOE Advanced Fuel-Cell Commercialization Working Group. Presented at the International Symposium on Combustion July 29.

Larminie, K. and Dicks, A. (2003). Fuel cell systems explained, Second Edition, John Wiley, England.

Lin, Y. and Beale, S (*2003*). Performance predictions in solid oxide fuel cells**.** *Third International Conference on CFD in the Minerals and Process Industries CSIRO, Melbourne, Australia 10-12 December*

Molenda, J. (*2006*). High-temperature solid-oxide fuel cells new trends in materials research. *Materials Science-Poland, 24 (1).312-325*

Noren, D. A. and Hoffman, M. A. (2005). Clarifying the Butler–Volmer equation and related approximations for calculating activation losses in solid oxide fuel cell models, J. Power Sources, 152 (5), Dec. 175–181.

O'M Bockris, J; Dandapani, B; Cocke, D. and Ghoroghchian, J. (1985). On the splitting of water. *Int. J. Hydrogen Energy,* 10 (30). 179-201.

Rosendahl, L.A; Mortensenand, P. V. and Enkeshafi, A.A. (2011). Hybrid solid oxide fuel cell and thermoelectric generator for maximum power output in micro-CHP systems. Journal of Electronic Materials, 40 (5), 2011DOI: 10.1007/s11664-011-1552-x. 431-453

Singhal, S. C. and Kendall, K. (2003). High temperature solid oxide fuel cells: Fundamentals, design and applications, Elsevier, Oxford, UK. Boalsburg, PA 16827. http://www.7ms.com/fct/index.html ccn/archive/archive.html#afn 2012. Assessed on 11th April, 2011. 113-145.

Singhal, S.C. (2000). Science and technology of solid-oxide fuel cells. *MRS Bulletin*, 25 **.** 16-21.

Stambouli, A. B. and Traversa, E. (2002). Solid oxide fuel cells (SOFCs): A review of an environmentally clean and efficient source of energy. Renewable and Sustainable Energy Reviews 6 (2). 433–455. www.elsevier.com/locate/rser. Assessed on 21th November, 2011.

Venkatasubramanian, R; Siivola, E; Colpitts, T. and O'Quinn, B. (2001). Thin-film thermoelectric devices with high room-temperature figures of merit, Nature. 4 (3). 597–602.

Westinghouse Electric Corporation, Bechtel Group, Inc; (1992). Solid oxide fuel cell repowering of high grove station unit 1, Final report, prepared for Southern California Edison Research Center, March.

Williams, M.C. (1999). Status of solid oxide fuel cell development and commercialization in the U.S, in *roc. 6th Internl. Symp. On Solid Oxide Fuel Cells*, Eds. S.C. Singhal and M. Dokiya, Electrochem. Soc., 3..

Winkler, W. (2003). *Thermodynamics*, in h*igh temperature solid oxide fuel cells: Fundamentals, Design and Applications*, S.C. Singhal and K. Kendall, Editors. Elsevier Ltd.: Oxford, UK. 53 - 82

World Energy Council (WEC). (1998). Survey of energy resources.. Fuel Data Center and the Clean Cities Program. http://www.eere.energy.gov/cleancities/. Assessed on 21th November, 2011.

Nomenclature

η	efficiency
ΔE	potential difference produced by a concentration change at the electrode called the concentration polarization
ΔG_r	reversible available energy change
ΔH_{rrevv}	reversible enthalpy change
μ_i	chemical potential
C_b	bulk concentration of reactant
C_s	concentration at the triple-phase boundary (tpb), where the gas, electrolyte, and electrode meet
E	electromotive force (emf)
E_{rev}	reversible electromotive force
E_{therm}	thermal electromotive force (voltage)
F	Faraday's constant
F	Faraday's constant
H	enthalpy of the system
i	current
I	current in Ampere
I_0	exchange current
L	limiting
n	number of moles of electrons participating in the reaction
n_i	species in moles
N^{in}	input mole flow rate

N^o output mole flow rate
N^r mole flow rate reacted
P partial pressure
P pressure
p_a ambient pressure in Pascals
Q the activity of terms of the reactants and products, each raised to its stoiochiometric coefficient.
R universal gas constant
T fuel cell temperature
T operating temperature of the fuel cell in Kelvins
t time in seconds
T temperature in Kelvins
$T\Delta S_r$ reversible energy loss
T_{fc} minimum fuel cell temperature constant
$T\Delta S$ system energy loss
U internal enery of the system
V voltage
V volume of water input
V_{act} activation loss
V_{con} concentration loss
V_{ohmic} ohmic loss.
W work done on the system
x species for the fuel cell
z charge on the particle or number of excess electrons
α_a coefficient of anode charge transfer
α_c coefficient of cathode charge transfer
β fuel cell maximum temperature constant
γ resistance in ohms
$\Delta G/dG$ change in available energy
ΔH change in enthalpy
ΔU change in internal energy
Δv change in volume
η_e thermoelectric conversion efficiency of the elements.
η_h ratio of heat flux through the elements in the modules to that from the inner shell to outer shell
η_{he} efficiency of heat exchange of the generator
ϕ the field under consideration

iafor